Published in final edited form as:
Nature. 2012 November 8; 491(7423): 249–253. doi:10.1038/nature11516.

Genetic programs constructed from layered logic gates in single cells

Tae Seok Moon[1,†], **Chunbo Lou**[1], **Alvin Tamsir**[2], **Brynne C. Stanton**[1], and **Christopher A. Voigt**[1]

[1]Synthetic Biology Center, Department of Biological Engineering, Massachusetts Institute of Technology, Cambridge, Massachusetts 02139, USA

[2]Tetrad Graduate Program, University of California San Francisco, San Francisco, California 94158, USA

Abstract

Genetic programs function to integrate environmental sensors, implement signal processing algorithms and control expression dynamics[1]. These programs consist of integrated genetic circuits that individually implement operations ranging from digital logic to dynamic circuits[2–6], and they have been used in various cellular engineering applications, including the implementation of process control in metabolic networks and the coordination of spatial differentiation in artificial tissues. A key limitation is that the circuits are based on biochemical interactions occurring in the confined volume of the cell, so the size of programs has been limited to a few circuits[1,7]. Here we apply part mining and directed evolution to build a set of transcriptional AND gates in *Escherichia coli*. Each AND gate integrates two promoter inputs and controls one promoter output. This allows the gates to be layered by having the output promoter of an upstream circuit serve as the input promoter for a downstream circuit. Each gate consists of a transcription factor that requires a second chaperone protein to activate the output promoter. Multiple activator–chaperone pairs are identified from type III secretion pathways in different strains of bacteria. Directed evolution is applied to increase the dynamic range and orthogonality of the circuits. These gates are connected in different permutations to form programs, the largest of which is a 4-input AND gate that consists of 3 circuits that integrate 4 inducible systems, thus requiring 11 regulatory proteins. Measuring the performance of individual gates is sufficient to capture the behaviour of the complete program. Errors in the output due to delays (faults), a common problem for layered circuits, are not observed. This work demonstrates the successful layering of orthogonal logic gates, a design strategy that could enable the construction of large, integrated circuits in single cells.

We designed the architecture of an AND gate according to two constraints (Fig. 1a). First, the gate needs to consist of parts that can be diversified to build multiple orthogonal gates. Second, the inputs and outputs of the gate should have a common signal carrier that enables

Correspondence and requests for materials should be addressed to C.A.V. (cavoigt@gmail.com).
†Present address: Department of Energy, Environmental & Chemical Engineering, Washington University in St Louis, St Louis, Missouri 63130, USA.

Supplementary Information is available in the online version of the paper.

Author Contributions T.S.M. designed and performed the experiments, analysed the data, developed the computational models and wrote the manuscript. C.L. developed the computational models. A.T. analysed the data. B.C.S. performed experiments. C.A.V. designed experiments, analysed the data, developed the computational models and wrote the manuscript.

The authors declare no competing financial interests.

them to be layered (the output of one serves as the input to the next)[8]. For transcriptional circuits, the inputs and the outputs are promoters. We have designed a transcriptional 2-input AND gate, in which one input promoter drives the expression of an activator and the second input promoter drives the expression of a chaperone protein. The chaperone is required by the activator to turn on the output promoter (Fig. 1b). Both proteins need to be expressed for the transcription factor to be active. The output promoter is therefore active only when both input promoters are active.

The transcription factors and chaperones were gleaned from gene clusters encoding type III secretion systems, which are found in many pathogenic bacteria[9]. One of the best characterized is encoded within *Salmonella* Pathogenicity Island 1 (SPI-1)[10].Within this island, a genetic circuit has been identified that regulates the expression of proteins that are exported by the system through a feedback mechanism mediated by protein–protein interactions between effectors, a chaperone (SicA) and a transcription factor (InvF) (Fig. 1c)[11]. The SicA–InvF complex activates transcription from the *sicA* promoter. Thus, SPI-1 provides three parts that can form the core of an AND gate: the activator, the chaperone and the inducible promoter.

The genes associated with the T3SS are encoded together within a genomic cluster. This simplifies the identification of sets of three of the parts that are likely to function together. Of more than 1,000 prokaryotic genomes in NCBI, 64 species have InvF homologues. We selected three genomes from which to glean parts: *Shigella flexneri*, *Yersinia enterocolitica* and *Pseudomonas aeruginosa*. The homologues share 27% (MxiE)[12], 15% (YsaE)[13] and 10% (ExsA)[14] identity with InvF. The SicA homologues are 54% (IpgC), 50% (SycB) and 13% (ExsC) identical. The *Pseudomonas* system has a different mechanism, involving three proteins and a partner-swapping mechanism[14]. The InvF and SicA homologues from each organism were codon-optimized for *E. coli* and synthesized. The *Salmonella*, *Shigella* and *Pseudomonas* parts had to be modified before their performance characteristics (orthogonality and dynamic range) were sufficient for incorporation into gates (Fig. 2a). The *Yersinia* parts were non-functional and were not pursued further.

The first *invF* gene we synthesized was based on the amino acid sequence from the annotated *Salmonella typhimurium* genome (AE006468).However, when co-expressed with *sicA*, it failed to activate the psicA promoter (Fig. 2b, ‘Annotated InvF’). This was corrected by determining that the gene was misannotated and is translated from an upstream ATG that adds 33 amino acids (Fig. 2b, ‘Correct InvF’).

Other changes had to be made to improve the dynamic ranges of the gates. Wild-type pipaH has a high basal background and is only induced threefold (Fig. 2c). A saturation mutagenesis library was designed to change the −10 region and screened to identify a mutant with a decreased background and higher dynamic range (Fig. 2a). A mutant was identified (pipaH*) that decreased the background and increased the dynamic range to 13-fold (Fig. 2c).

Of the six possible non-cognate protein–protein interactions that could exhibit crosstalk, only one was found to be significant. The SicA chaperone induced the MxiE transcription factor (Fig. 2d). Error-prone PCR was applied to *sicA*, and the library was screened for mutants that decreased crosstalk with MxiE but maintained the ability to induce InvF (Supplementary Information). A SicA mutant (SicA*) containing a single F62Y mutation was identified that decreased the activation of MxiE to 2.6-fold, while retaining wild-type 70-fold activation of InvF (Fig. 2d).

The engineered parts from each system were then tested for orthogonality. The first potential for crosstalk is at the level of interaction between activators and chaperones (Fig. 2e). The SicA, IpgC and ExsC chaperones were able to activate their cognate systems 87-fold, 14-fold and 34-fold, respectively, and the off-target effects were minimal (Supplementary Fig. 4). The second possibility for crosstalk was on the level of the interaction between the transcription factor and the promoter (Fig. 2f). To test this, we co-expressed each cognate activator–chaperone pair and measured the ability of the complex to activate the three promoters (Supplementary Fig. 4). As with the protein–protein interactions, strong induction was observed only between cognate parts.

The sets of parts from each organism were assembled to form three 2-input AND gates (Fig. 3). To characterize each gate, two input promoters were chosen that were induced by small molecules: arabinose (pBAD) and aTc (pTet) for *Salmonella/Shigella* and AI-1 (pLux*) and aTc (pTet*) for *Pseudomonas* (Fig. 3a). The output promoter of each gate was transcriptionally fused to red fluorescent protein (RFP). The AND gates based on InvF-SicA*, MxiE-IpgC and ExsDA-ExsC showed 73-fold, 14-fold and 33-fold induction, respectively (Fig. 3b). These AND gates can be converted to NAND gates (providing a Boolean complete function) through the addition of a NOT gate[4]. We demonstrated this by connecting the *Salmonella* AND gate to a new NOT gate based on the PhlF repressor, which yields a 13-fold inverted response (Supplementary Fig. 6).

A problem with the gate characterization is that the data are presented where the input is an inducer concentration and the output is fluorescence. To guide the connection of circuits, the data need to be in a form in which the inputs and the outputs have the same units. This was achieved by using a mathematical model combined with additional experiments (Supplementary Information). The activity of the promoter of each inducible system was characterized independently and was fitted to a simple thermodynamic model (Supplementary Figs 7 and 8). This formed the basis on which to parameterize a model of each AND gate such that the inputs and outputs were the activities of the respective promoters (Fig. 3c). To report the data in relative expression units (REUs)[15], the activities were normalized by the activity of a constitutive promoter, as measured with the same fluorescent reporter (Supplementary Fig. 15)[16].

The 2-input AND gates were designed to be layered to create more complex programs. We constructed 3-input and 4-input AND gates through different permutations of the 2-input gates (Fig. 4). There are alternative logic combinations, some much simpler, that would produce the same functions; these particular designs were chosen with the purpose of studying gate layering. The inputs into these programs were promoters that were activated by small-molecule inducers. In both cases, the output of the program was on only when all of the inducers were present in the medium. For the 3-input gate, the output when all inducers were present [111] was 4.5-fold above the highest off state [011] (Fig. 4b). For the 4-input gate, the output when all the inducers are present [1111] was 5.1-fold above the highest off state [1011] (Fig. 4e). The dynamic behaviour was characterized for the induction and relaxation of the 4-input program by switching between the [0000] and [1111] states (Fig. 5a). The 4-input AND gate represents a large genetic program that requires connecting 7 genetic devices (3 gates and 4 inducible systems) and includes 11 regulatory proteins, making it the largest and most complex program constructed so far[7].

A key question is whether characterization data for individual circuits is sufficient to predict the performance of a program. This assumption could be false as a result of differences in the genetic context, interference between circuits, or a combined impact on cellular resources[17,18]. To test this, we used the data obtained for the individual gates (Fig. 3c) and the inducible systems (Supplementary Fig. 8) to calculate the expected response of the

programs. This was then compared with the measured values (Fig. 4b, e). Both programs behaved as expected for all of the input states (Fig. 5b).

A potential problem in layering genetic logic gates is that the resulting programs are asynchronous[19]. In other words, there is no clock that synchronizes the progression of the signal between gates. Because there are delays at each layer, this can lead to transient errors in the output, known as faults[20]. This is a well-studied phenomenon in electronic systems. A fault can occur when a signal is divided and then one branch skips a layer (for example, in Fig. 4a the pTet input signal skips the first layer). Because the on signal reaches the next layer faster than the other, the gate at the second layer will transiently respond to the wrong state of input signals. This phenomenon is related to pulses that can occur in incoherent feedforward loops in signalling networks[21].

Genetic programs composed of layered transcriptional circuits could be susceptible to faults because there can be delays between layers (about 20–40 min)[22] and the dynamics of each circuit consists of mixed timescales[21]. A simple kinetic model was used to determine the condition for faults to occur (Supplementary Information). Considering an AND gate consisting of two proteins *x* and *y*, large faults occur when the delay time

$$t_{\mathrm{d}} >> \frac{\gamma_x \gamma_y}{K \alpha_x \alpha_y \gamma_{\mathrm{g}}},$$

where *K* is the association constant of *x* and *y* to each other and DNA, α is the expression rate, γ is the degradation rate and γ_g is the degradation rate of the reporter protein. For typical values (K = 0.001 nM^{-2}, α = 10 nM min^{-1} and γ_g = 0.01 min^{-1}), avoiding a fault due to a 30-min delay (about one layer) requires degradation half-times to be faster than about 20 min. When binding cooperativity is included, this further decreases the magnitude of the fault.

We designed experiments to measure faults that could occur in the 3-input and 4-input AND gates. In particular, the 3-input gate (Fig. 4a) has the potential for a fault when shifting from a +Ara/+IPTG/−aTc [110] to a [011] state (removal of Ara and addition of aTc). Both of these states should correspond to an off output, so when the inputs are changed, the output should stay off. However, there is the potential for a fault because the pTet inducible system could turn on faster than the first AND gate (MxiE-IpgC) turns off. There is also the potential for the SicA* protein to persist if it were to degrade slowly, even after the gate has been turned off. Thus, a fault would occur and the output (RFP) would be expressed until the first gate is inactivated and SicA* degrades. No such fault is observed when cells are shifted between these input states (Fig. 5c). This implies that the chaperones degrade more quickly than the transcription factors are expressed. Similar experiments with the 4-input gate (Fig. 5d) also failed to show any faults. This may become a larger issue as the size of the program and the number of circuits increases, which could yield higher-order effects on the cell[23].

This work represents the design of genetic circuits with the intent to be scalable; in other words, an underlying architecture chosen to use part classes can easily be diversified to build orthogonal gates. Part mining proved valuable to expand the number of gates, but it was also necessary to apply directed evolution to tune their properties functionally. Once characterized, the circuits were combined in different permutations to build programs. The largest program required 11 regulatory proteins and 38 additional genetic parts, all of which were encoded in 21 kilobases on three plasmids. Building larger integrated circuits will require new tools, including computer-aided design[24], a better understanding of how circuits

interact with each other and affect the host[17,25], and methods to minimize the impact of environment, evolution and genetic context on circuit performance.

METHODS SUMMARY

Strains, plasmids and growth media

E. coli DH10B was used for all the experiments and grown in Luria–Bertani (LB) medium (Miller, BD Biosciences). Kanamycin (20 μg ml^{-1}), ampicillin (100 μg ml^{-1}) and chloramphenicol (34 μg ml^{-1}) were added as appropriate. Four inducers were obtained from Sigma Aldrich: Ara (Arabinose), IPTG (isopropyl β-D-1-thiogalactopyranoside), 3OC6 (*N*-(β-ketocaproyl)-L-homoserine lactone) and aTc (anhydrotetracycline). All the newly constructed plasmids were made by the one-step isothermal DNA assembly method as described previously[26].

Part mutagenesis

Promoter regions were modified by saturation mutagenesis. To construct the promoter libraries, the bases were randomized by using oligonucleotides (Integrated DNA Technologies) as shown in Supplementary Fig. 3. After PCR reactions, the blunt ends were ligated with T4 DNA ligase (New England BioLabs) to give the mixture of the modified plasmids. To obtain *sicA* variants, error-prone PCR was performed. Random mutations were introduced by PCR reactions with 1 × PCR buffer supplemented with 7 mM $MgCl_2$, 0.3 mM $MnCl_2$, 0.2 mM dATP, 0.2 mM dGTP, 1 mM dCTP, 1 mM dTTP and 0.05 U *Taq* DNA polymerase (Invitrogen). The detailed methods including library screening are described in Supplementary Methods.

Flow cytometry

E. coli was grown overnight in LB medium at 37 °C and then transferred to fresh LB medium in 96-well plates (USA Scientific). Each culture (0.6 ml) was induced at a D_{600} of 0.5 (unless otherwise specified) with inducers of different concentrations as indicated, and flow cytometer data were obtained using an LSRII flow cytometer (BD Biosciences). All the data were gated by forward and side scatter, and each data consists of at least 10,000 cells. The arithmetic mean fluorescence was calculated with FlowJo (TreeStar Inc.), and the averages of means were obtained from three replicates performed on different days.

Supplementary Material

Refer to Web version on PubMed Central for supplementary material.

Acknowledgments

C.A.V. is supported by Life Technologies, Defense Advanced Research Projects Agency Chronicle of Lineage Indicative of Origins (DARPA; CLIO N66001-12-C-4018), the Office of Naval Research (N00014-10-1-0245), the National Science Foundation(NSF;CCF-0943385), the National Institutes of Health (AI067699) and the NSF Synthetic Biology Engineering Research Center (SynBERC; SA5284-11210). The content of the information does not necessarily reflect the position or the policy of the Government, and no official endorsement should be inferred.

References

1. Khalil AS, Collins JJ. Synthetic biology: applications come of age. Nature Rev. Genet. 2010; 11:367–379. [PubMed: 20395970]
2. Lucks JB, Qi L, Mutalik VK, Wang D, Arkin AP. Versatile RNA-sensing transcriptional regulators for engineering genetic networks. Proc. Natl Acad. Sci. USA. 2011; 108:8617–8622. [PubMed: 21555549]

3. Anderson JC, Voigt CA, Arkin AP. Environmental signal integration by a modular AND gate. Mol. Syst. Biol. 2007; 3:133. [PubMed: 17700541]
4. Wang B, Kitney RI, Joly N, Buck M. Engineering modular and orthogonal genetic logic gates for robust digital-like synthetic biology. Nature Commun. 2011; 2:508. http://dx.doi.org/10.1038/ncomms1516. [PubMed: 22009040]
5. Danino T, Mondragon-Palomino O, Tsimring L, Hasty J. A synchronized quorum of genetic clocks. Nature. 2010; 463:326–330. [PubMed: 20090747]
6. Basu S, Mehreja R, Thiberge S, Chen MT, Weiss R. Spatiotemporal control of gene expression with pulse-generating networks. Proc. Natl Acad. Sci. USA. 2004; 101:6355–6360. [PubMed: 15096621]
7. Purnick PE, Weiss R. The second wave of synthetic biology: from modules to systems. Nature Rev. Mol. Cell Biol. 2009; 10:410–422. [PubMed: 19461664]
8. Canton B, Labno A, Endy D. Refinement and standardization of synthetic biological parts and devices. Nature Biotechnol. 2008; 26:787–793. [PubMed: 18612302]
9. Galan JE, Collmer A. Type III secretion machines: bacterial devices for protein delivery into host cells. Science. 1999; 284:1322–1328. [PubMed: 10334981]
10. Galan JE, Curtiss R. Cloning and molecular characterization of genes whose products allow *Salmonella typhimurium* to penetrate tissue culture cells. Proc. Natl Acad. Sci. USA. 1989; 86:6383–6387. [PubMed: 2548211]
11. Darwin KH, Miller VL. Type III secretion chaperone-dependent regulation: activation of virulence genes by SicA and InvF in *Salmonella typhimurium*. EMBO. J. 2001; 20:1850–1862. [PubMed: 11296219]
12. Mavris M, Sansonetti PJ, Parsot C. Identification of the *cis*-acting site involved in activation of promoters regulated by activity of the type III secretion apparatus in *Shigella flexneri*. J. Bacteriol. 2002; 184:6751–6759. [PubMed: 12446624]
13. Walker KA, Miller VL. Regulation of the Ysa type III secretion system of *Yersinia enterocolitica* by YsaE/SycB and YsrS/YsrR. J. Bacteriol. 2004; 186:4056–4066. [PubMed: 15205407]
14. Thibault J, Faudry E, Ebel C, Attree I, Elsen S. Anti-activator ExsD forms a 1:1 complex with ExsA to inhibit transcription of type III secretion operons. J. Biol. Chem. 2009; 284:15762–15770. [PubMed: 19369699]
15. Temme K, Zhao D, Voigt CA. Refactoring the nitrogen fixation gene cluster from *Klebsiella oxytoca*. Proc. Natl Acad. Sci. USA. 2012; 109:7085–7090. [PubMed: 22509035]
16. Kelly JR, et al. Measuring the activity of BioBrick promoters using an *in vivo* reference standard. J. Biol. Eng. 2009; 3:4. [PubMed: 19298678]
17. Tan C, Marguet P, You L. Emergent bistability by a growth-modulating positive feedback circuit. Nature Chem. Biol. 2009; 5:842–848. [PubMed: 19801994]
18. Arkin A. Setting the standard in synthetic biology. Nature Biotechnol. 2008; 26:771–774. [PubMed: 18612298]
19. Harold A, et al. Amorphous computing. Commun. ACM. 2000; 43:74–82.
20. Katz, RH.; Borriello, G. Contemporary Logic Design. Prentice Hall: 1994.
21. Mangan S, Alon U. Structure and function of the feed-forward loop network motif. Proc. Natl Acad. Sci. USA. 2003; 100:11980–11985. [PubMed: 14530388]
22. Hooshangi S, Thiberge S, Weiss R. Ultrasensitivity and noise propagation in a synthetic transcriptional cascade. Proc. Natl Acad. Sci. USA. 2005; 102:3581–3586. [PubMed: 15738412]
23. Cookson NA, et al. Queueing up for enzymatic processing: correlated signaling through coupled degradation. Mol. Syst. Biol. 2011; 7:561. [PubMed: 22186735]
24. Clancy K, Voigt CA. Programming cells: towards an automated ‘Genetic Compiler’. Curr. Opin. Biotechnol. 2010; 21:572–581. [PubMed: 20702081]
25. Del Vecchio D, Ninfa AJ, Sontag ED. Modular cell biology: retroactivity and insulation. Mol. Syst. Biol. 2008; 4:161. [PubMed: 18277378]
26. Gibson DG, et al. Enzymatic assembly of DNA molecules up to several hundred kilobases. Nature Methods. 2009; 6:343–345. [PubMed: 19363495]
27. Marlovits TC, et al. Structural insights into the assembly of the type III secretion needle complex. Science. 2004; 306:1040–1042. [PubMed: 15528446]

28. Temme K, et al. Induction and relaxation dynamics of the regulatory network controlling the type III secretion system encoded within *Salmonella* pathogenicity island 1. J. Mol. Biol. 2008; 377:47–61. [PubMed: 18242639]

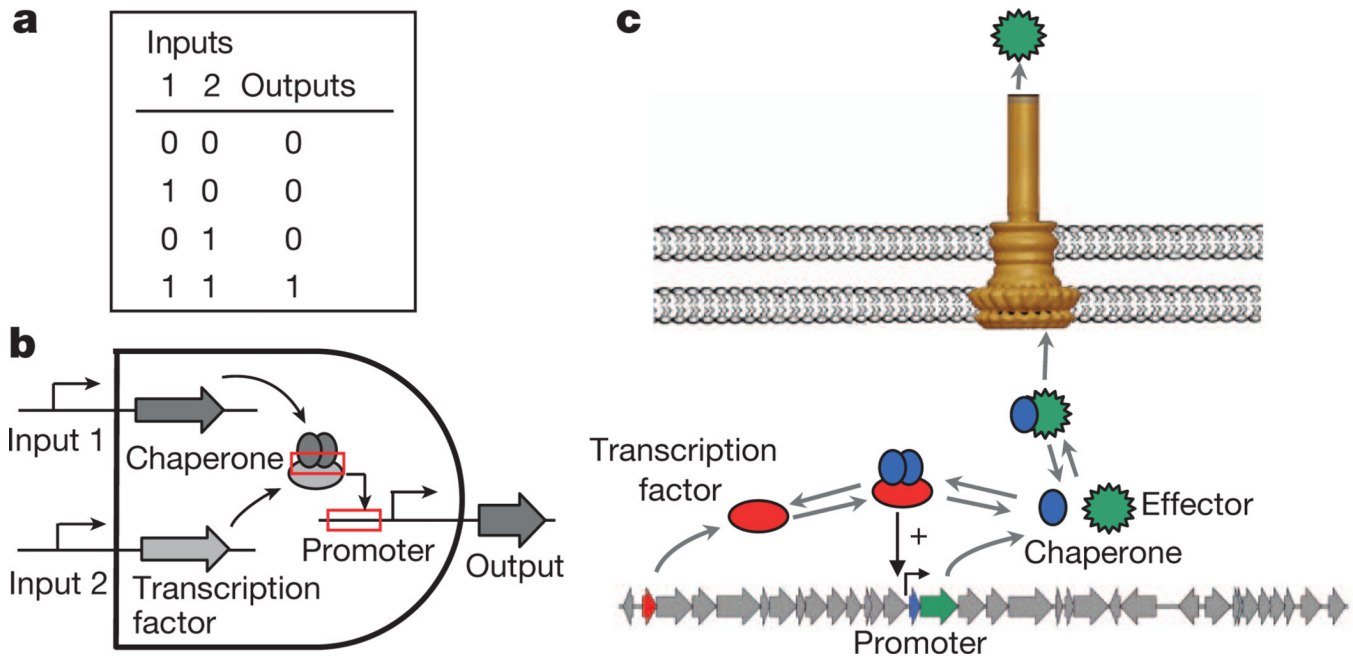

Figure 1. Mining circuits from genomic islands

a, The truth table for an AND gate. **b**, The architecture of an AND gate. The protein–protein and protein–DNA interactions that can lead to crosstalk between gates are shown as red rectangles. **c**, The gene cluster from SPI-1 and the needle structure[27,28]. The transcription factor InvF is shown in red, the chaperone SicA in blue, and the SipC effector in green.

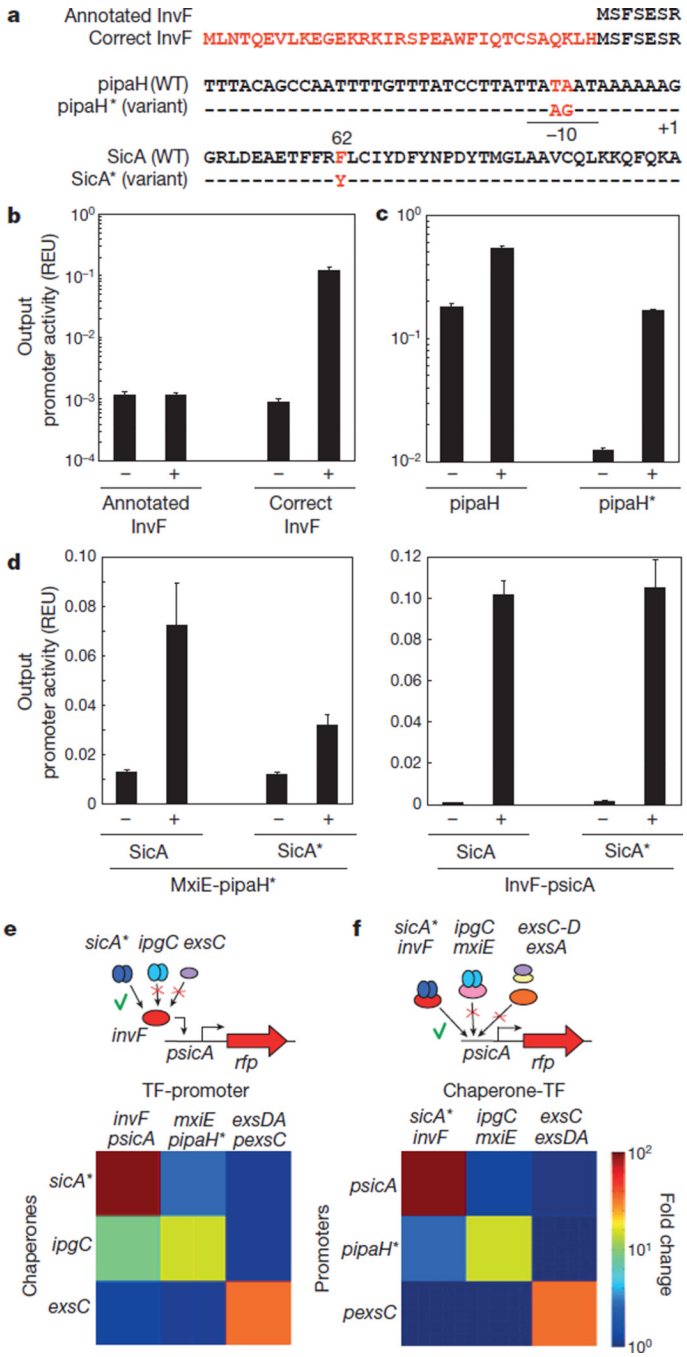

Figure 2. Part engineering to improve dynamic range and orthogonality

a, Sequences for the InvF activator (top), the pipaH promoter variant (middle) and the SicA mutant (bottom). **b**, A comparison in the induction of the psicA promoter by the short (annotated) and long (correct) InvF sequences. **c**, A comparison of the wild-type and mutant (pipaH*) promoters. **d**, A comparison of the wild-type and mutant (SicA*) chaperones. Activation of either the pipaH* promoter by MxiE (left) or the psicA promoter by InvF (right) is shown. In **b–d** the chaperone (SicA and IpgC) and activator (InvF and MxiE) are expressed from the pBAD and pTet promoters, respectively: −, no inducer; +, 5 mM Ara and 50 ng ml^{-1} aTc. **e**, The orthogonality of protein–protein interactions. This figure shows the

fold change, calculated by dividing the fluorescence values (with both inputs on) by the minimum fluorescence from each promoter (with both inputs off). The inducers were 5 mM Ara for *sicA** and *ipgC*, 1 μM 3OC6 for *exsC*, and 50 ng ml^{-1} aTc for *invF*, *mxiE* and *exsDA*. **f**, The orthogonality of protein–DNA interactions. All of the error bars in these figures were calculated as the s.d. of three replicates performed on different days. The error bars for **e** and **f** are shown in Supplementary Fig. 4.

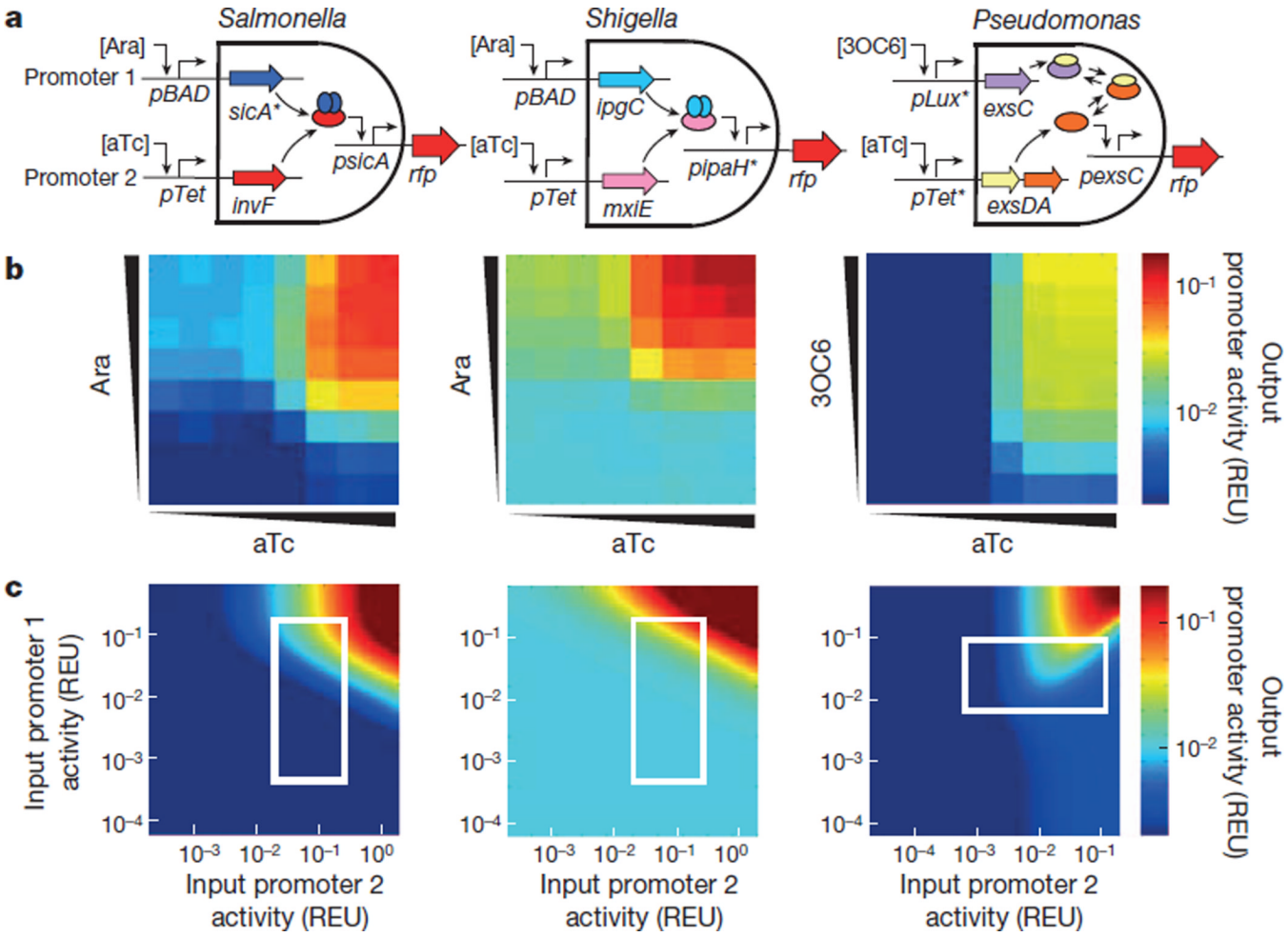

Figure 3. Three 2-input AND gates constructed using *Salmonella* (left), *Shigella* (middle) and *Pseudomonas* (right) parts

a, The architecture of three AND gates. **b**, The transfer functions obtained by measuring fluorescence. The inducers used were Ara (0, 0.0016, 0.008, 0.04, 0.2, 1, 5 and 25 mM) and 3OC6 (0, 0.32, 1.6, 8, 40, 200, 1,000 and 5,000 nM) from bottom to top; and aTc (0, 0.0032, 0.016, 0.08, 0.4, 2, 10 and 50 ng ml^{-1}) from left to right. Data are averages of three replicates performed on different days. **c**, The transfer functions as fitted to mathematical models. The white boxes show the experiment ranges obtained by the inducible promoters. Note that **b** and **c** cannot be visually compared to determine the goodness of the fit because the axes are rescaled. Supplementary Fig. 10 shows a quantitative comparison, which yields an R^2 of 0.9.

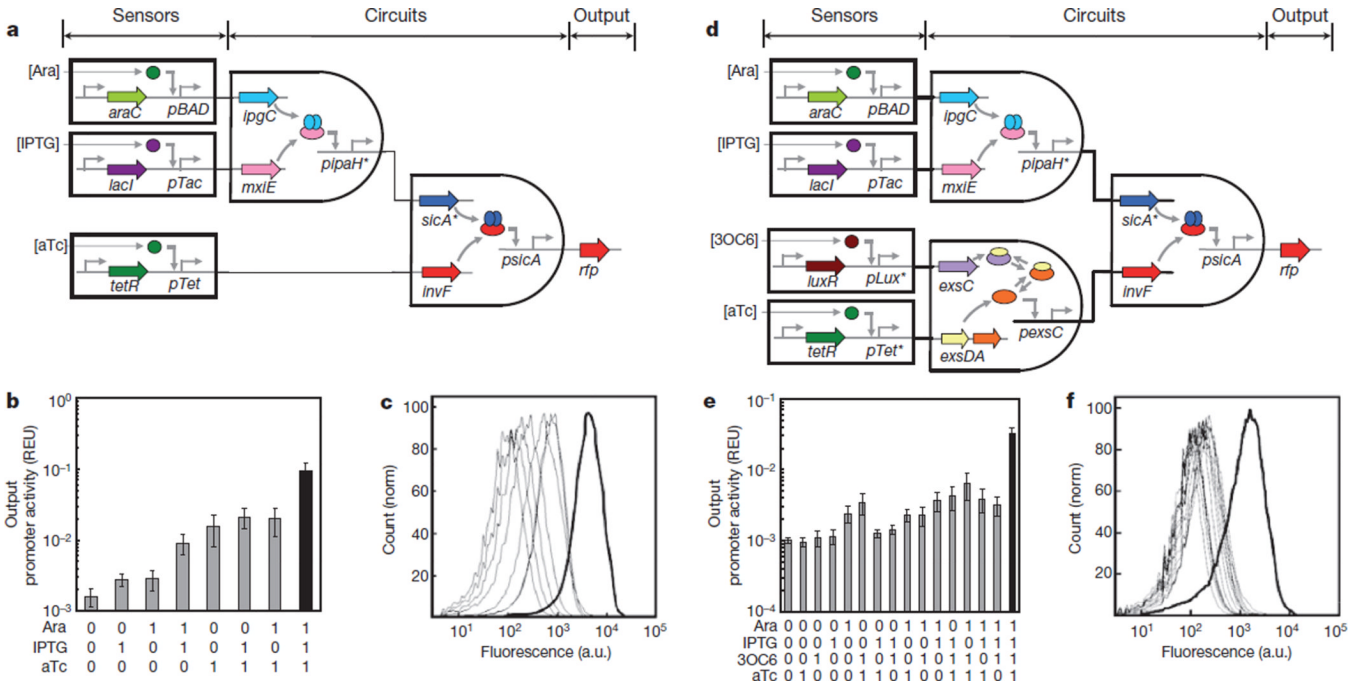

Figure 4. Genetic programs formed by layering AND gates

a, 3-input AND gate. This system consists of three sensors, an integrated circuit and a reporter gene. **b**, The fluorescence measured from cells containing the 3-input AND gate. The three inducers used for the on (1) input are Ara (5 mM), IPTG (0.1 mM) and aTc (10 ng ml^{-1}). Data are means and s.d. for three replicates performed on different days. **c**, Raw cytometry data for all sets of input states. The thick line is for the [111] set of inducers. **d**, 4-input AND gate. **e**, The output fluorescence for different combinations of inputs. The four inducers used for the on input were Ara (5 mM), IPTG (0.1 mM), 3OC6 (5 μM) and aTc (10 ng ml^{-1}). **f**, Raw cytometry data for all input states. The thick line is for [1111].

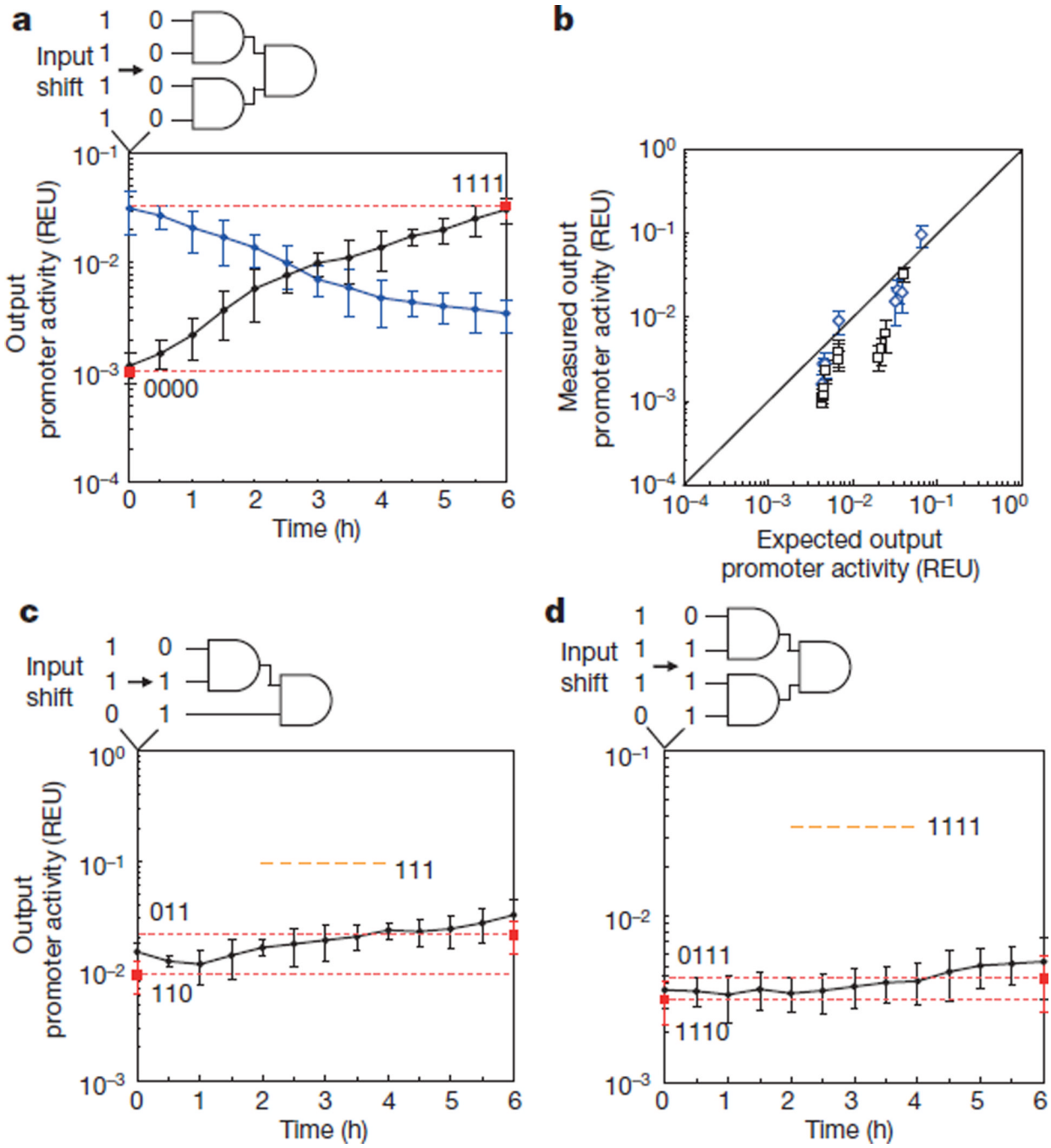

Figure 5. Performance of genetic programs

a, The dynamic behaviour for the induction and relaxation of the 4-input program. The input states were switched either [0000] to [1111] (at D_{600} = 0.25; black diamonds) or [1111] to [0000] (at D_{600} = 0.05; blue diamonds). The off and on states are shown as a reference (red dashed lines, values from Fig. 4). **b**, A comparison for the output 'expected' from combining the independently measured transfer functions of each gate with that 'measured' in the final context. Each data point is from a different combination of inducers for the 3-input (blue diamonds) and 4-input (black squares) programs. The line shown is $y = x$. **c**, The dynamic behaviour for the 3-input gate switching from [110] to [011] (at D_{600} = 0.25). The input

states are listed as [Ara IPTG aTc]. **d**, The dynamic behaviour for the 4-input gate switching from [1110] to [0111]. The input states are listed as [Ara IPTG 3OC6 aTc]. The four inducer concentrations used for the on input for the 3- and 4-input AND gate were Ara (5 mM), IPTG (0.1 mM), 3OC6 (5 μM) and aTc (10 ng ml^{-1}). The on state is shown as a reference (orange dashed lines). The red dashed lines indicate the steady-state outputs for the corresponding inputs (Fig. 4). The error bars show s.d. calculated on the basis of three replicates performed on different days.